DCEA Disaster in Civil Engineering and Architecture

POPULAR SCIENTIST

Research Article

# Investigation of Seismic Performance of Double-Angle Braces with Single Lacing under Two-Step Variable-Amplitude Cyclic Loading

Arief Panjaitan[a,*], Yulia Hayati[a], Helfisa Ikram[b], Purwandy Hasibuan[a], Rudiansyah Putra[a], Surya Bermansyah[a], Muhammad Fauzi[a], Muhammad Haiqal[c], Masaru Shimizu[d]

[a]Civil Engineering Department, Faculty of Engineering, Universitas Syiah Kuala, Darussalam, Banda Aceh 23111, Indonesia

[b]Civil Engineering Master's Program, Faculty of Engineering, Universitas Syiah Kuala, Darusalam, Banda Aceh 23111, Indonesia

[c]Architecture and Planning Department, Faculty of Engineering, Universitas Syiah Kuala, Darussalam, Banda Aceh 23111, Indonesia

[d]Civil Engineering Department, Nagoya University, Furo-Cho, Chikusa-Ku, 464-8603, Japan

***Corresponding Author:** Arief Panjaitan (arief_panjaitan@usk.ac.id)

**Articles History:** **Received:** 20 August 2026; **Revised:** 28 September 2026; **Accepted:** 18 October 2026; **Published:** 7 November 2026

Copyright © 2026 A. Panjaitan et al. This is an open access article distributed under the terms of the Creative Commons Attribution-NonCommercial 4.0 International License (CC BY-NC 4.0), which permits any non-commercial use, distribution, and reproduction in any medium, provided the original author(s) and source are properly cited.

**Publisher's Note:** *Popular Scientist* stays neutral with regard to jurisdictional claims in published maps and institutional affiliations.

## Abstract

Aceh Province, which is located in an earthquake-prone area, requires an earthquake-resistant structure, i.e., a Concentrically Braced Frame System (CBFs). The CBFs have brace elements installed diagonally on the structure, and it reduces horizontal displacement in the structure due to the earthquake. This study implemented several Two-Step Variable Amplitude (TSVA) loading histories, consisting of two cyclic uniform load blocks with low and high amplitudes, which represent a simplification of earthquake loads due to amplitude changes. The test was conducted by installing the CBF brace in the loading frame and applying the TSVA parallelly with long axis of the brace. The experimental study yielded that the CBF brace with the largest cyclic ranges exhibited the highest strength, stiffness, and dissipated energy. Furthermore, the braces tested under TSVA with less uniform repeated cycles exhibited better strength, stiffness, and dissipated energy, which corresponds to the smaller fatigue effect in the CBF brace, thereby enhancing their seismic capability. Observing the failure modes of the CBF brace indicated that all the specimens experienced flexural buckling due to the TSVA loading histories.

**Keywords:** Concentrically Braced Frame, CBF Braces, Two-Step Variable Amplitude, Seismic Capabilities, Fatigue Effect

## Introduction

The Concentrically Braced Frame System (CBFs) is a structural system designed to strengthen buildings, especially for those located in earthquake-hazard areas. CBFs consist of a main frame and braced elements installed diagonally on the structural frame. So far, several studies have been conducted

to observe the behavior and to strengthen the CBFs. Several studies elaborated on the seismic performance of Buckling Restrained Braces (BRB) installed in Concentrically Braced Frames (CBFs) by conducting shaking table tests on 10-story steel` CBFs, presenting an original nonlinear comparative study of BRB frames and Eccentrically Braced Frames (EBF) under column-removal scenarios, proposing a novel self-centering dual-stage yielding BRB, and then comparing it with those incorporating a conventional self-centering brace and a conventional buckling-restrained brace, and evaluating large-scale pseudo-dynamic hybrid simulations on different ductile steel braced frame systems, including a Buckling-Restrained Braced Frame (BRBF), a Special Concentrically Braced Frame (SCBF), a Yielding Brace System (YBS) equipped with cast steel Yielding Connectors (YCs), and EBFs designed with Cast Steel Replaceable Modular Yielding Links (CMLs) [1-5].

Other studies made a combination of brace and damper systems to improve the seismic capabilities of CBFs by revealing the optimal configuration of bracing CBF-damper systems and establishing Hybrid Bracing Systems (HBs) [6-8]. Several research works also attempted to discover seismic behavior of Special Concentrically Braced Frames (SCBFs), which have better ductility than that of ordinary CBFs, by varying the plastic hinge locations of steel SCBF structures and evaluated the modification of an existing 13-story hotel building into an SCBF system and found that the SCBF-modified structure satisfies the minimum 90% mass participation requirement specified in SNI 1726:2019, with the SCBF system achieving this criterion using fewer vibration modes [9-10]. In the past, several studies combined the Moment Resisting Frame (MRF), EBF, and CBF to increase the seismic capabilities of structures by evaluating displacement and drift of the systems; assessing the influence of pulses of near-fault ground excitations (NFGEs) on lateral story and inter-story displacements in buildings of different heights of EBFs and CBFs, and establishing fragility curves originating from Eccentrically Inverted V Brace Frames (EBFs) and CBFs [11-13].

Several studies also evaluated the seismic behaviour of the CBF braces to obtain the behavior of the energy-dissipating element, where the studies were conducted by evaluating two different sections of CBF braces: the IWF section and the double-channel sections to improve the seismic capabilities of CBFs, and compared the seismic performance of multi-storey buildings with CBF using HSS and WF profiles as bracing elements by using Nonlinear static pushover analysis. [14-15]. In separate studies, discussions on the Steel Chevron and Split-X CBFs were also elaborated by investigating the various design parameters that affect the seismic response of CBFs and improving the prediction of internal forces in non-dissipative members of Chevron and Split-X CBFs [16-17].

Mohamed & Rad [18] studied the seismic performance by enhancing the Steel Knee-Braced Frames through Optimization of Knee Length and Supplemental Supports. Li et al. [19] developed a constitutive model for a Self-centering Brace (SCB), implemented and validated its numerical simulation using OpenSees. Morales and Baez [20] developed two-dimensional models for nonlinear time–history analysis (NLTHA), employing scaled real accelerograms, conventional

gravity loads, and detailed numerical models. Rafiee et al. [21] examined the lateral behaviour of two 12-storey modular buildings, where steel modules serve as the Gravity Force-Resisting System (GFRS), and either a CBF or a reinforced concrete shear wall acts as the Seismic Force-Resisting System (SFRS). Elettore [22] presents the design and preliminary experimental testing of an isolated brace equipped with Friction Devices (FDs) for steel CBFs.

The research mentioned above has not yet elaborated on the seismic capabilities of the brace under variability of amplitudes. This study discussed the seismic capabilities of double braces under different ranges of TSVA (variable amplitude) loading histories. Here, the double section is an alternative to strengthen the brace. Next, the seismic capabilities were investigated to reveal the brace behavior, and observations were made of the failure mode. The expected contribution is the seismic brace behavior for design purposes and the effectiveness of the double brace in improving seismic performance.

## Experimental Program

### Detail of Specimens

The object of study is the CBF brace, which is constructed from double steel angles. In this study, the material properties of the steel CBF brace are obtained from the coupon tensile test, as shown in Figure 1 and Table 1.

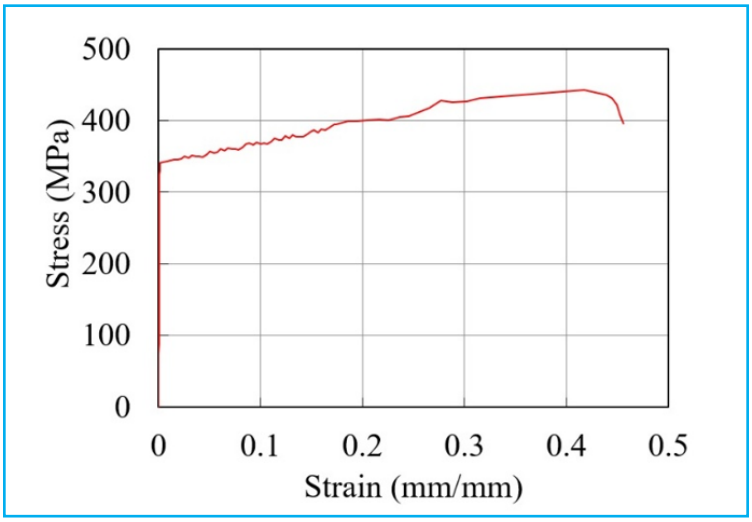



**Figure 1.** Stress-strain relationships of the CBF brace

**Table 1.** Material properties of CBFs brace

| Component | Grade | Yield strength (MPa) | Tensile strength (MPa) | Elasticity modulus (MPa) | Elongation (%) |
|---|---|---|---|---|---|
| CBF brace | A572 | 336 | 442 | 204112 | 45 |

Table 1 expresses the material model. The constitutive model was a kinematic hardening rule based on true stress-strain relationships, with Et/E = 0.0034 (E and Et are the initial elastic slope and the second-slope plastic phase).

To obtain the yield displacement required for the TSVA, a double-section brace model was first established and simulated under tensile monotonic loading using Abaqus v.6.14. All specimens were 1500 mm long and modeled using S4R5 shell elements, with six degrees of freedom per node (three translational and three rotational). The S4R5 element was selected to capture the required nodal degrees of freedom and prevent rigid-body motion. A mesh convergence study was performed to determine an appropriate mesh size. To ensure accurate results while minimizing computational time, an element aspect ratio (length-to-width) of approximately 1.0 was adopted, as shown in Figure 2. Lacing was used as the connector, with its cross-sectional area based on the laboratory specimens and defined in the Abaqus Profile feature. Tensile loading was applied to determine the yield displacement, as illustrated in Figure 2(a).

For the analysis, the double-angle compressive members were fully fixed at the lower end, while the upper sectional-area mesh was constrained to a reference point (RP), as shown in Figure 2(a) and 2(b). Tensile loading was incrementally applied through the RP using the RIKS procedure to capture the nonlinear static response. Due to the applied load, the material experienced geometrical imperfections, i.e., elongation. The applied tensile load and corresponding upper-end displacement were recorded at each increment to determine the yield point. The yield point is located at the transition region from the elastic to plastic phase in the load-axial elongation relationship (capacity curve). From the capacity curve, it was obtained that the yield displacement ($1\delta_y$) was 0.5 mm. Later, $1\delta_y$ was utilized to determine the real amplitude of TSVA and was implemented throughout the test. The validation of the analysis-test for obtaining $1\delta_y$ was not required since $1\delta_y$ was merely used as the amplitude unit for implementing TSVA to the specimen in the experiment.

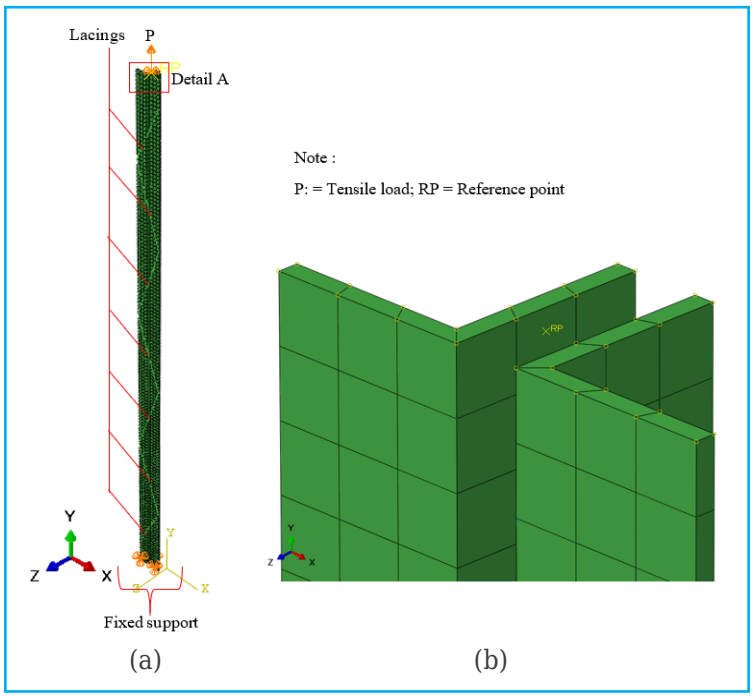



**Figure 2.** CBF brace modelling and simulation. (a) Tensile load application, (b) Detail A: Model meshing and tie constraint to connect node region and reference point (RP).

To construct the steel double angle-brace, several single lacing plates were used and linked to the steel angle by a welded connection. In the experiment, both ends of all braces are connected to the gusset plate by a bolted connection. There are three test specimens (CBF braces) tested in the laboratory, with the specimen details and its cross sectional view are illustrated in Figures 3 and 4. In this study, each test specimen was subjected to several different loading histories (TSVA) as shown in Table 2.

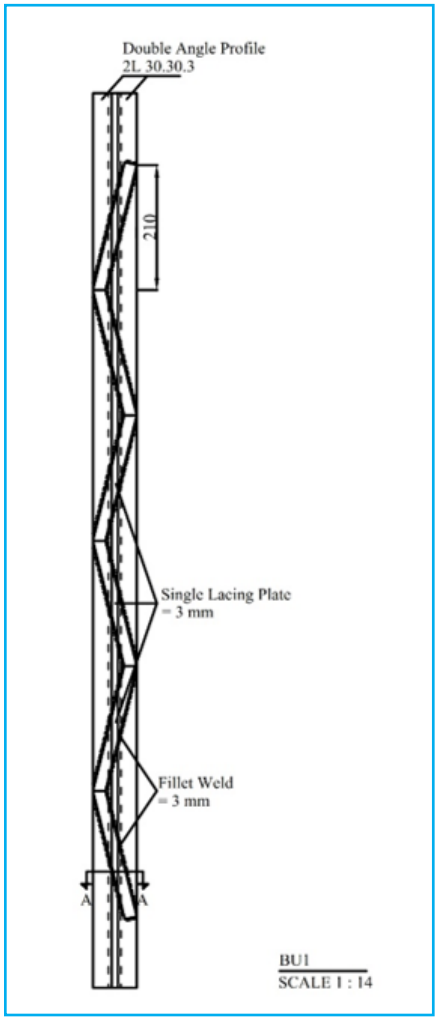



**Figure 3.** Specimens details (unit: mm)

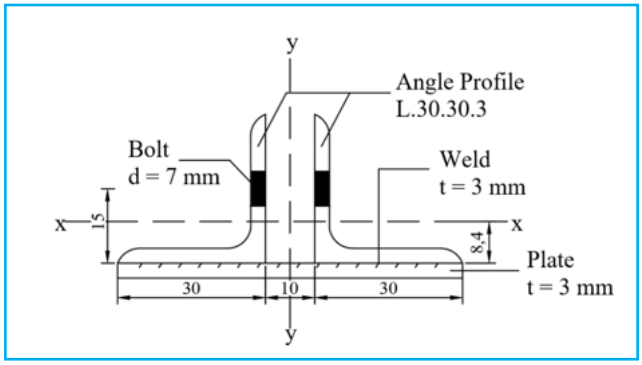


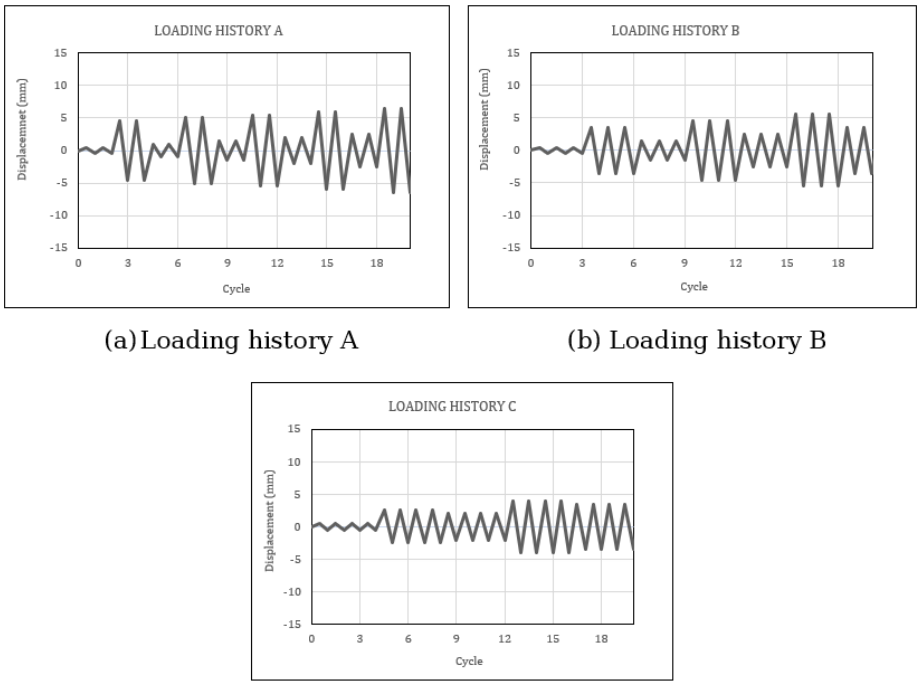

**Figure 4.** Cross-sectional A-A (unit: mm)

**Table 2.** Specimen characteristics subjected to several different loading histories (TSVA)

| No | Specimens name | Loading history type |
|---|---|---|
| 1 | BU1A | A |
| 2 | BU1B | B |
| 3 | BU1C | C |

### *Two-Step Variable Amplitude Loading*

The unit used for the TSVA loading history is yield displacement because the CBF structure is affected by earthquakes, where the effects of large displacement are due to the ground shaking. Experimental work was carried out by applying the three TSVAs to the brace specimens. The cyclic displacement ranges and the number of cyclic loading repetitions in a block of TSVA distinguished these loading histories. Figure 5 and Tables 3, 4, and 5 present the TSVA illustrations.




(a) Loading history A (b) Loading history B

(c) Loading history C

**Figure 5.** Loading histories of TSVA illustrations

**Table 3.** Loading history A of TSVA illustrations

| Block | Amplitude type | Amplitude value ($\delta_y$) | Amplitude value (mm) | Number of cycles |
|---|---|---|---|---|
| 1 | Low | 1 | 0.5 | |
| 2 | High | 9 | 4.5 | |
| 3 | Low | 2 | 1.0 | The number of cycles for |
| 4 | High | 10 | 5.0 | each block is 2 cycles |
| 5 | Low | 3 | 1.5 | |
| etc | | | | |

**Table 4.** Loading history B of TSVA illustrations

| Block | Amplitude type | Amplitude value ($\delta_y$) | Amplitude value (mm) | Number of cycles |
|---|---|---|---|---|
| 1 | Low | 1 | 0.5 | |
| 2 | High | 7 | 3.5 | |
| 3 | Low | 3 | 1.5 | The number of cycles for each block is 3 cycles |
| 4 | High | 9 | 4.5 | |
| 5 | Low | 5 | 2.5 | |
| etc | | | | |

**Table 5.** Loading history C of TSVA illustrations

| Block | Amplitude type | Amplitude value ($\delta_y$) | Amplitude value (mm) | Number of cycles |
|---|---|---|---|---|
| 1 | Low | 1 | 0.5 | |
| 2 | High | 5 | 2.5 | |
| 3 | Low | 4 | 2 | The number of cycles for each block is 4 cycles |
| 4 | High | 8 | 4 | |
| 5 | Low | 7 | 3.5 | |
| etc | | | | |

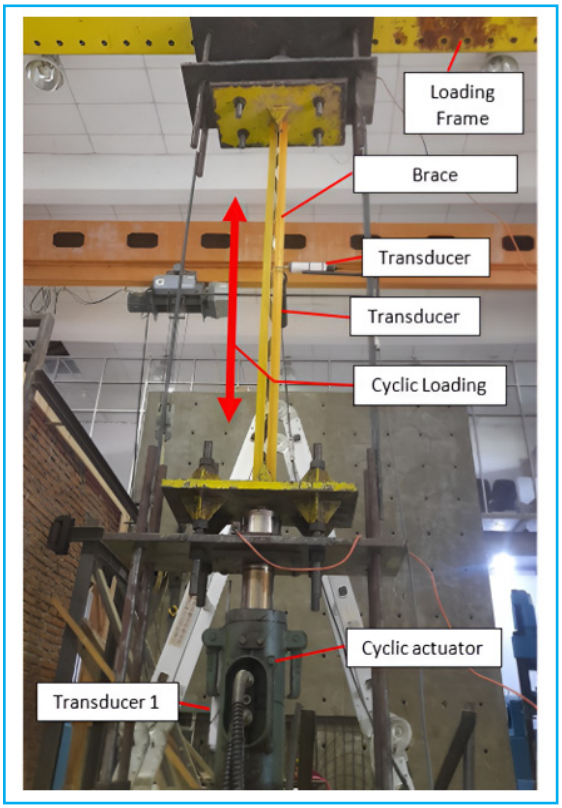



**Figure 6.** Test setup of Two-Step Variable Amplitude (TSVA) loading histories

### *Test Setup*

The testing was conducted in accordance with the setup as shown in Figure 6. The cyclic load was applied following the TSVA loading histories using a cyclic actuatorh. The displacement control speed was set between 0.001 and 0.05 mm/sec. Transducer 1 was placed under the supporting plate to measure the

cyclic displacement occurring. Meanwhile, transducers 2 and 3 were mounted on the body and legs of the angle profile to monitor the possibility of bending deformation along the angle section axis. Both transducers (transducers 2 and 3) were located at the midpoint of the brace length, where initial bending is supposedly to occur.

The test was conducted by first applying a tensile load until the yield point was reached, where the yield deformation in the tensile direction was used as the displacement control. After reaching the yield deformation, the test continued with the application of compressive displacement.

The recorded data includes load and displacement values for each loading cycle. These recordings produced a hysteretic curve that shows the relationship between load and displacement. From this hysteresis curve, the capability of the single-plate lacing brace can be revealed, including its strength, stiffness, and dissipated energy. Additionally, the failure modes of each specimen were also discussed to verify the influence of cyclic displacement ranges and the number of cyclic repetitions in a block on the TSVA to specimen strength.

## Results and Discussions

### Hysteretic Curves

To identify the specific behavior of the test specimen under cyclic loading, the initial stage presents the load-displacement curve (hysteresis curve) after one cycle passes the yielding point ($1\delta_y$), as shown in Figure 7. During the elastic condition, the load-displacement relationship remains linear for the three test specimens. When cyclic loading was applied beyond the yield condition, the tensile load was continued until reaching the ultimate load. After the ultimate load was reached, the loading was continued in the compressive direction (unloading) until reaching the ultimate load in compression. For one cycle, the loading is continued until the displacement returned to zero (0).

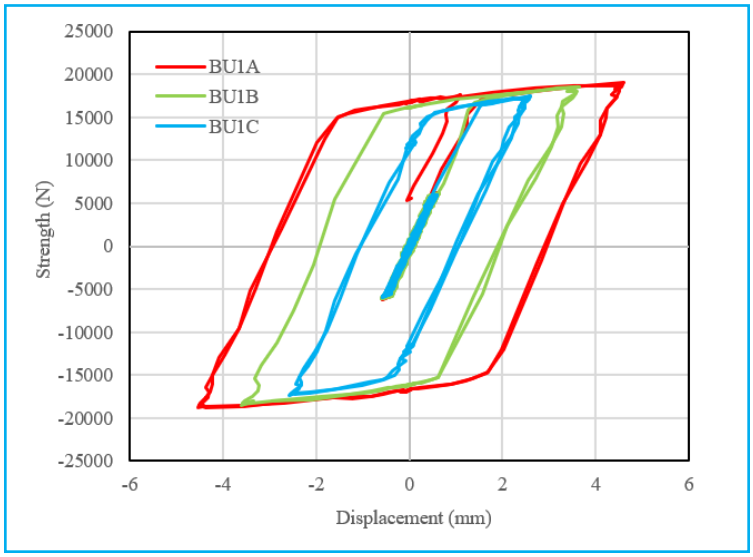



**Figure 7.** Load-displacement relationships of double brace specimens for one cycle under TSVA loading histories (Type A, B, and C) obtained from the experiment

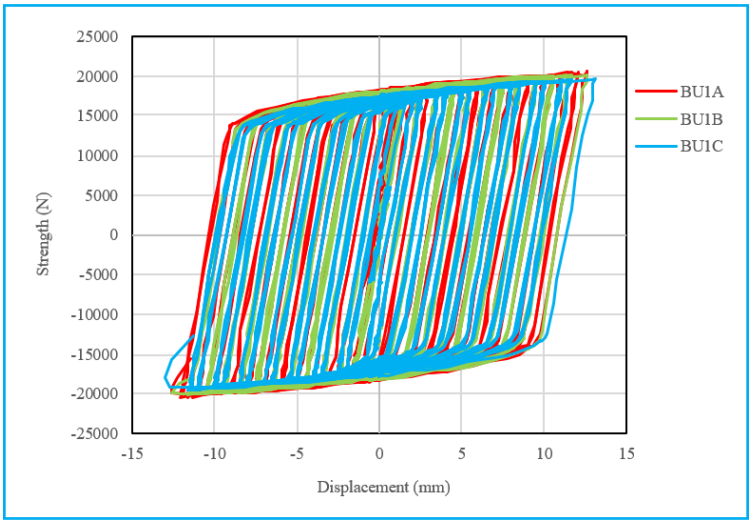



**Figure 8.** Comparison of double brace hysteretic curves under TSVA loading histories (Type A, B, and C) until the failure of the specimens obtained from the experiment

Figure 8 shows the results of cyclic load testing on several CBF brace specimens with a length of 1500 mm under TSVA loading histories until the test specimens' failure. From the figure, it can be seen that BU1A shows the highest strength compared to BU1B and BU1C. This finding indicates that the smaller the number of cyclic repetitions in a block of TSVAs yield greater the strength of the brace specimens. This can be observed in Figure 8, where BU1A, with the fewest number of cycles (2 cycles per block), exhibits the highest strength at the same displacement compared to BU1B and BU1C (3 and 4 cycles per block) in both tensile and compressive strengths. An increase in the number of cycles leads to strength degradation, meaning that the more cycles a block of TSVA undergoes, the lower the strength will be at the same displacement. This finding also indicates that the specimen experienced fatigue conditions where the strength tended to be reduced due to more cyclic repetitions. Additionally, among the three test specimens, the increase in strength is more significant under elastic conditions compared to plastic conditions.

The strength of the test specimens, namely the ultimate strength values of BU1A, BU1B, and BU1C in tension, are 20514.972 N, 20281.364 N, and 19756.096 N, respectively. Meanwhile, the maximum displacements of BU1A, BU1B, and BU1C are 12.6 mm, 12.598 mm, and 13.1 mm.

### *Tensile and Compressive Strength*

Figures 9 and 10 show the tensile and compressive strength values for each cycle for the three different loading histories. From these two figures, it can be seen that there are differences in each test specimen for cycle repetition in terms of compressive and tensile strength. The specimens tested under a smaller number of cycle repetitions in a block of TSVA show higher strength compared to specimens tested under more cycle repetitions in a block of TSVA at the same cyclic displacement.

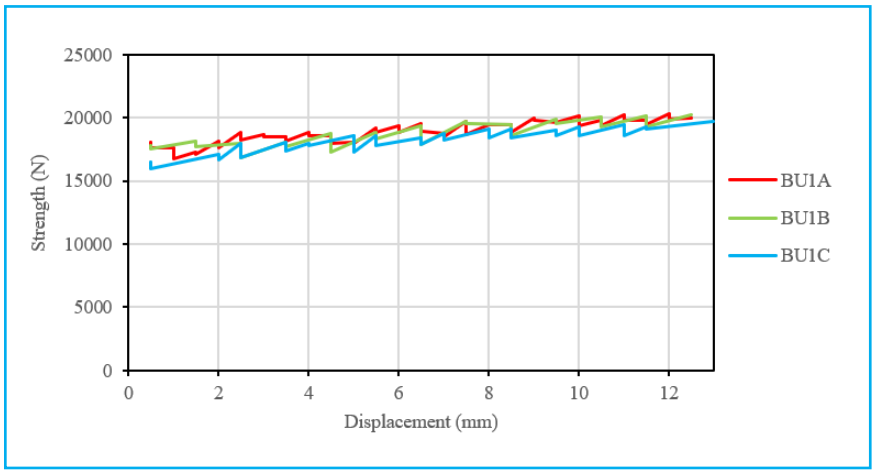



**Figure 9.** Tensile strength of the test specimen

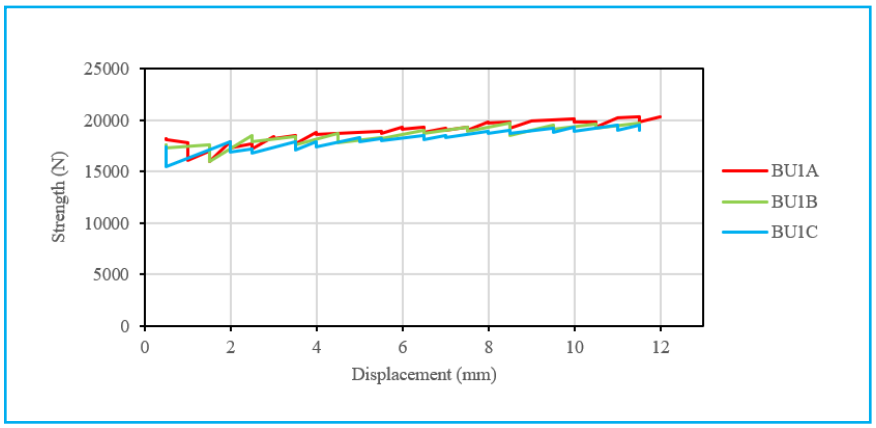



**Figure 10.** Compressive strength of the test specimen

Figures 9 and 10 show the difference in the effect of cycle repetition on the tensile and compressive strength of the brace on BU1A with 2 cycle repetitions, BU1B with 3 cycle repetitions, and BU1C with 4 cycle repetitions in a block of TSVA. From the figures, the strength of BU1A was higher than those of BU1B and BU1C at the same cyclic displacement since BU1A was simulated under a smaller number of cyclic load repetitions in a block than those of BU1B and BU1C. The smaller number of cyclic repetitions tended to perform smaller fatigue effect in the brace. Thus, the higher strength on BU1A was presented.

Based on those figures, the tensile strength and compressive strength values of all test specimens show similarity. This indicates that the test specimens exhibit isotropic properties of steel.

### *Tensile and Compressive Stiffness*

Figures 11 and 12 show the tensile and compressive stiffness for each displacement cycle of the three loading history variations. From these two figures, it can be seen that there are differences in compressive and tensile stiffness between test specimens due to differences in the number of cycles applied.

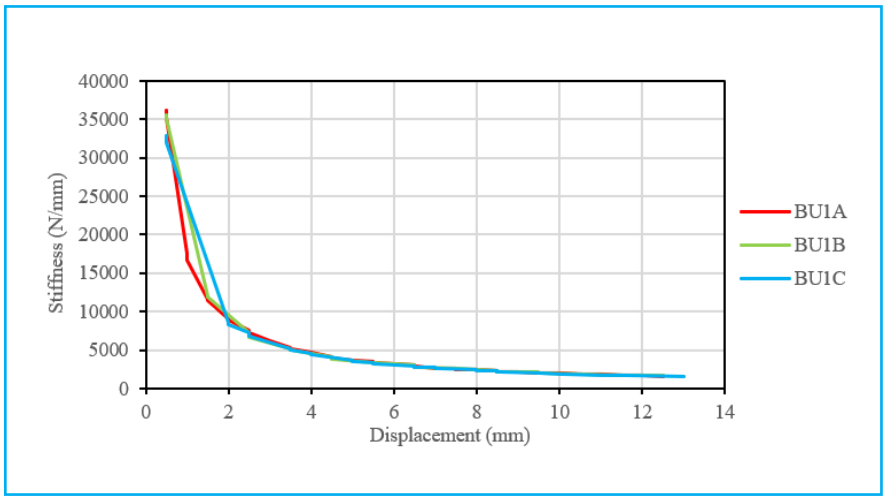



**Figure 11.** Tensile stiffness of the test specimen

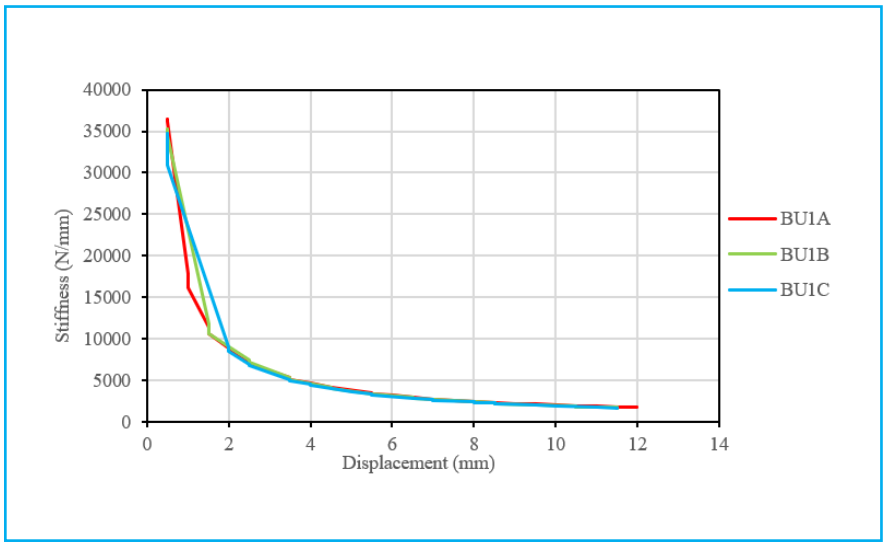



**Figure 12.** Compressive stiffness of the test specimen

From the figure, it can be seen that in the 0-2 mm interval (BU1B and BU1C) with more cycle repetitions in one block, the stiffness value is smaller than that of BU1A. This is possible because BU1B and BU1C do not have displacement amplitude values in the 0-2 mm interval. Therefore, in that range, the stiffness values are expressed in a linear distribution.

### *Dissipated Energy*

The dissipated energy was calculated when the cycle exceeded $1\delta_y$. Cumulative energy dissipation at low amplitudes is influenced by energy dissipation from high amplitudes, so low-amplitude energy dissipation shows a more significant increase.

Figure 13 shows that a single-lacing brace with low amplitude shows a more significant increase in cumulative dissipation energy compared to high amplitude. This is influenced by the previous high-amplitude cycle, so that the accumulation of energy in the low-amplitude cycle shows a more significant increase.

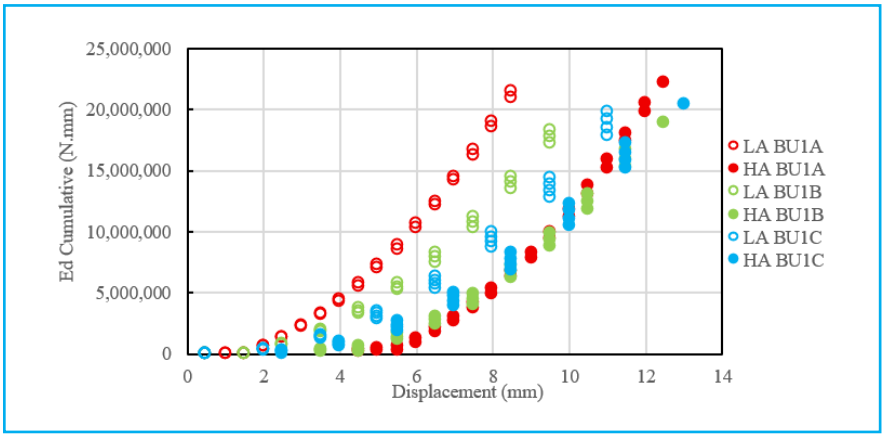



**Figure 13.** Dissipated energy of test specimen

### *Failure Modes*

Figure 14 shows the failure modes of CBF brace specimens due to the implementation of TSVA loading histories. Based on the figure, it can be seen that the type of buckling that occurs is flexural buckling. This shows that the additional cross-section of the brace can reduce the possibility of buckling, such as buckling modes in the single-section brace, i.e., local, torsional, or flexural-torsional buckling.




**Figure 14.** Failure mode of double brace under TSVA loading histories. (a) Front view of specimen. (b) Side view of specimen

**Table 6.** The results data of the double brace with a single lacing plate connector

| Specimen | Pu (N) | δu1 (mm) | δu2 (mm) | δu3 (mm) | Number of cycles until failure |
|---|---|---|---|---|---|
| BU1A | 20,514.972 | 12.600 | 107.281 | 1.912 | 67 |
| BU1B | 20,281.364 | 12.598 | 110.638 | 2.072 | 58 |
| BU1C | 19,756.096 | 13.100 | 120.421 | 2.363 | 61 |

Table 6 presents the results of the double brace under TSVA loading histories. In this test, 3 (three) main displacement points were observed, namely $\delta_{u1}$, $\delta_{u2}$, and $\delta_{u3}$. From the data, it can be seen that BU1A shows a higher load value (20,514.971 kN) than BU1B and BU1C. This is influenced by the greater number of cycles in BU1A (67 cycles) and also influenced by fewer cyclic repetitions in a block of TSVA (2 cycles) until failure than in BU1B and BU1C.

## Conclusion

Based on the discussion and capability measurement of the double brace under the TSVA loading histories, the capability of the test specimen with loading history A was better than that of the other test specimens. The strength of the double brace with loading history A was greater than that of the double brace with loading histories B and C, with differences of 1.14% and 3.70%, respectively. The higher strength of the double brace under loading history A is exhibited due to fewer cyclic loading repetitions than those of the double brace under loading histories B and C. The smaller number of cyclic loading repetitions will reduce the fatigue effect on the specimen. Thus, the strength tends to be higher than that of the other specimens, which is observed at the same cyclic displacement. The stiffness of the double brace with loading history A is greater than that of loading histories B and C, with differences of 1.66% and 9.02%, respectively. The energy dissipation of the double brace with loading history A is greater than that of loading histories B and C, with differences of 5.17% and 8.32%, respectively. Observing the failure modes of the brace specimens revealed that all specimens experienced flexural buckling, indicating that additional brace sections diminished the possibility of other buckling types, such as buckling due to the single-section brace.

## Acknowledgement

The authors would like to express their gratitude to Lembaga Penelitian dan Pengabdian Masyarakat (the Research and Community Service Board), LPPM of Universitas Syiah Kuala.

## Conflicts of Interest

The authors declare no conflict of interest.

## Author Contributions

**Arief Panjaitan:** conceptualization, methodology, investigation, formal analysis, writing-review & editing. **Yulia Hayati:** validation, supervision, writing-review & editing. **Helfisa Ikram:** investigation, writing-original draft. **Purwandy Hasibuan:** writing-review & editing. **Rudiansyah Putra:** writing-review & editing. **Surya Bermansyah:** writing-review & editing. **Muhammad Fauzi:** writing-review & editing. **Muhammad Haikal:** writing-review & editing. **Masaru Shimizu:** validation, supervision, writing-review & editing.

## Data Availability Statement

The data that support the findings of this study are available on request from the corresponding author.

## Declaration of Generative AI and AI-Assisted Technologies in the Writing Process

Not Applicable.

## References

[1] J. Fujiwara et al., "Full-scale Shaking Table Tests on a 10-story Steel Moment-resisting Frame Building with Buckling-restrained Braces," Earthquake Engineering & Structural Dynamics, Aug. 2026, doi: https://doi.org/10.1002/eqe.70202

[2] S. S. Mungase, M. T. Zope, and G. S. Supekar, "Study Of Minimum Tie Force Requirements on the Progressive Collapse Resistance of Steel Braced Frames," International Journal of Recent Advances in Engineering and Technology, vol. 15, no. 1, pp. 159-164, 2026, doi: doi: https://doi.org/10.65521/intjournalrecadvengtech.v15i1.2807

[3] P. H. Vishwe, D. V Bharitkar, and G. S. Supekar, "Comparative Nonlinear Analysis of Buckling Restrained Braced (BRB) And Eccentric Braced Frames (EBF) For Progressive Collapse Resistance Using ETABS," International Journal of Recent Advances in Engineering and Technology, vol. 15, no. 1, 2026, doi: https://doi.org/10.65521/intjournalrecadvengtech.v15i1.2809

[4] Q. Cheng, Y. Shi, H. Qin, and Y. Ding, "Seismic Performance of Concentrically Braced Steel Frames Equipped with Novel Self-Centering Dual-Stage Yielding Buckling-Restrained Braces," Buildings, vol. 16, no. 5, Mar. 2026, doi: https://doi.org/10.3390/buildings16050960

[5] P. Mortazavi, O. S. Kwon, and C. Christopoulos, "Challenges and Lessons Learned From Pseudo-Dynamic Hybrid Simulations on Ductile Steel Braced Frame Systems," Earthquake Engineering & Structural Dynamics, vol. 54, no. 4, pp. 1229–1250, Apr. 2025, doi: doi: http://dx.doi.org/10.1002/eqe.4301

[6] F. Xu et al., "Development and Seismic Performance Analysis of a Brace-Damper System in Steel Frame Structures," Structural Control and Health Monitoring, vol. 2026, no. 1, 2026, doi: https://doi.org/10.1155/stc/2122630

[7] R. V. Vasegh, M. Barghian, Y. Rahbar, and M. Abbaasi, "Seismic performance of a novel bracing system including cable-ring-arc together with MR damper in a steel frame," Scientific Reports, Jul. 2026, doi: https://doi.org/10.1038/s41598-026-58935-8

[8] A. J. Abdulridha, I. S. I. Harba, and A. A. M. Al-Shaar, "Seismic performance of steel frames with a hybrid bracing system combining concentric steel bracing and friction dampers," Fracture and Structural Integrity, vol. 20, no. 76, pp. 129–153, Apr. 2026, doi: https://doi.org/10.3221/IGF-ESIS.76.09

[9] H. Siahaan and D. A. Prabowo, "Efek Variasi Perilaku Sendi Plastis Pada Analisis Pushover Sistem Rbkk Tipe Inverted-V," Jurnal Mitra Teknik Sipil, vol. 9, no. 1, pp. 107-122, 2026, doi: https://doi.org/10.24912/jmts.v9i1.35823

[10] Y. Septiarsilia, E. Susanti, D. K. Fitriyah, D. Pertiwi, and U. Miron, "Seismic Performance Evaluation Of Building Structures Modified With Special Concentrically Braced Frames (SCBF)" Civilla: Jurnal Teknik Sipil Universitas Islam Lamongan, vol. 11, no. 1, pp. 77–88, 2026.

[11] Y. Septian Yoganata et al., “Comparative Seismic Performance Analysis of a 30-Story Building Structure with CFST Columns Using Concentrically Braced Frame and Moment Resisting Frame Systems,” Jurnal Aplikasi Teknik Sipil, vol. 24, no. 2, pp. 97-106, 2026.

[12] M. Yurdakul, Z. Tonyali, H. Sesli, and M. F. Farzam, “Effects of pulse-type near-fault ground motions on the nonlinear seismic response of steel frames with inverted-V CBF and EBF systems,” Scientific Reports, Jul. 2026, doi: https://doi.org/10.1038/s41598-026-62932-2

[13] H. H. Hasan and W. M. Arif, “Comparative Study of Steel Buildings with Eccentrically Inverted V-Brace Frames and Concentrically Inverted V-Brace Frames,” Civil and Environmental Engineering, Jun. 2026, doi: https://doi.org/10.2478/cee-2026-0066

[14] A. Panjaitan, Y. Hayati, R. Asmaijar, and M. Shimizu, “Seismic Performance of IWF and Double-channel Bracings in CBF Systems under Random Variable Amplitude Loading,” Disaster in Civil Engineering and Architecture, vol. 3, no. 1, pp. 45–55, Feb. 2026, doi: https://doi.org/10.70028/dcea.v3i1.74

[15] N. Ambarwati, R. Aidil Fitrah, M. Masrilayanti, and Z. Al Jauhari, “The comparative study between HSS and WF section as braced toward seismic performance of concentrically braced frame in multi-storey steel building,” in E3S Web of Conferences, EDP Sciences, Dec. 2025, doi: https://doi.org/10.1051/e3sconf/202567706009

[16] M. Bosco and P. P. Rossi, “Design Internal Forces of Non-Dissipative Members in CBFs With Regular and Irregular Brace Configurations,” Earthquake Engineering & Structural Dynamics, 2026, doi: https://doi.org/10.1002/eqe.70252

[17] B. Mahmoudi and A. Imanpour, “Seismic Design of Steel Chevron and Split-X Concentrically Braced Frames,” Earthquake Engineering & Structural Dynamics, vol. 54, no. 10, pp. 2565–2585, Aug. 2025, doi: https://doi.org/10.1002/eqe.4372

[18] A. T. Mohammed and M. H. Adib Rad, “Seismic Performance Enhancement of Steel Knee-Braced Frames through Optimization of Knee Length and Supplemental Supports,” Civil and Environmental Engineering, 2026, doi: https://doi.org/10.2478/cee-2027-0006

[19] Y. Li, G. Fan, M. Wang, and Q. Tan, “Seismic Performance Analysis of Steel Frame Structures with Self-centering Braces Based on OpenSees,” Journal of Physics: Conference Series, vol. 3242, no. 1, p. 012028, May 2026, doi: https://doi.org/10.1088/1742-6596/3242/1/012028

[20] E. G. Morales and A. G. Haro-Báez, “Displacement Profile Equations for Performance-Based Seismic Design of Concentrically Braced Steel Frames,” Buildings, vol. 16, no. 3, Feb. 2026, doi: https://doi.org/10.3390/buildings16030665

[21] Ali. Rafiee, E. Bazarchi, A. Davaran, and C. P. Lamarche, “Seismic Behavior of Multi-Storey Volumetric Modular Buildings: Comparing Concentrically Braced Frames and Reinforced Concrete Shear Walls,” ce/papers, vol. 8, no. 6, pp. 1156–1161, Dec. 2025, doi: https://doi.org/10.1002/cepa.70205

[22] E. Elettore, A. B. Francavilla, S. Di Benedetto, M. Latour, F. Freddi, and G. Rizzano, “Experimental Response of Friction-Based Dissipative Braces for Steel Seismic-Resilient Concentrically Braced Frames,” ce/papers, vol. 8, no. 6, pp. 1121–1126, Dec. 2025, doi: https://doi.org/10.1002/cepa.70218